

Medical-VLBERT: Medical Visual Language BERT for COVID-19 CT Report Generation with Alternate Learning

Guangyi Liu, Yinghong Liao, Fuyu Wang, Bin Zhang, Lu Zhang, Xiaodan Liang, Xiang Wan, Shaolin Li, Zhen Li*, Shuixing Zhang and Shuguang Cui, *Fellow, IEEE*

Abstract—Medical imaging technologies, including computed tomography (CT) or chest X-Ray (CXR), are largely employed to facilitate the diagnosis of the COVID-19. Since manual report writing is usually too time-consuming, a more intelligent auxiliary medical system that could generate medical reports automatically and immediately is urgently needed. In this article, we propose to use the medical visual language BERT (Medical-VLBERT) model to identify the abnormality on the COVID-19 scans and generate the medical report automatically based on the detected lesion regions. To produce more accurate medical reports and minimize the visual-and-linguistic differences, this model adopts an alternate learning strategy with two procedures that are knowledge pretraining and transferring. To be more precise, the knowledge pretraining procedure is to memorize the knowledge from medical texts, while the transferring procedure is to utilize the acquired knowledge for professional medical sentences generations through observations of medical images. In practice, for automatic medical report generation on the COVID-19 cases, we constructed a dataset of 368 medical findings in Chinese and 1104 chest CT scans from The First Affiliated Hospital of Jinan University, Guangzhou, China, and The Fifth Affiliated Hospital of Sun Yat-sen University, Zhuhai, China. Besides, to alleviate the insufficiency of the COVID-19 training samples, our model was first trained on the large-scale Chinese CX-CHR dataset and then transferred to the COVID-19 CT dataset for further fine-tuning. The experimental results showed that Medical-VLBERT achieved state-of-the-art performances on terminology prediction and report generation with the Chinese COVID-19 CT dataset and the CX-CHR dataset. The Chinese COVID-19 CT dataset is available at <https://covid19ct.github.io/>.

Index Terms—COVID-19 Lesion diagnosis, Automatic Report Generation, Visual Language BERT, Imaging-based AI diagnosis

Guangyi Liu, Yinghong Liao and Fuyu Wang have equal contributions to this work.

Corresponding authors are Xiaodan Liang, Shuixing Zhang, Shaolin Li and Zhen Li. Zhen Li is the lead corresponding author.

Guangyi Liu, Yinghong Liao, Zhen Li and Shuguang Cui are with Shenzhen Research Institute of Big Data and Future Network of Intelligence Institute (FNii), the Chinese University of Hong Kong, Shenzhen 518172, China (e-mail: guangyiliu@link.cuhk.edu.cn, yinghongliao@link.cuhk.edu.cn, lizhen@cuhk.edu.cn, shuguangcui@cuhk.edu.cn).

Xiang Wan is with Shenzhen Research Institute of Big Data and Guangdong Provincial Key Laboratory of Big Data Computing, the Chinese University of Hong Kong, Shenzhen 518172, China (e-mail: wanxiang@sribd.cn).

Fuyu Wang and Xiaodan Liang are with Sun Yat-sen University, Guangzhou 510275, China (e-mail: wangfy8@mail2.sysu.edu.cn, xdliao328@gmail.com).

Bin Zhang and Shuixing Zhang are with Department of radiology, the First affiliated hospital of Jinan University, Guangzhou 510630, China (e-mail: 1297225541@qq.com, shui7515@126.com).

Lu Zhang is with Jinan University, Guangzhou 510632, China (e-mail: zl2019@stu2019.jnu.edu.cn).

Shaolin Li is with the Fifth Affiliated Hospital of Sun Yat-sen University, Zhuhai 519000, China (e-mail: lishlin5@mail.sysu.edu.cn).

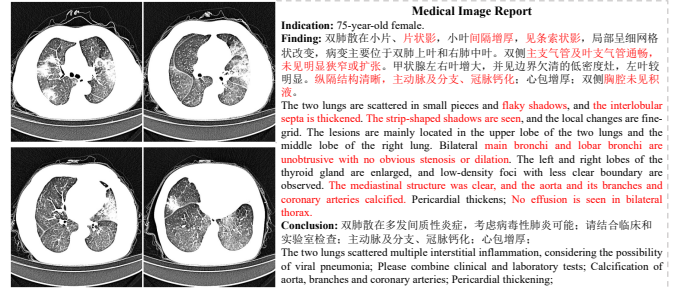


Fig. 1. Example of the COVID-19 medical image report in Chinese. The medical terminologies in findings are marked red. The intelligent system for automatic medical report generation needs to employ these terminologies accurately to offer radiologists a report template with the details of individual lesions, e.g., shape, density and boundary. With the template, radiologists can not only quickly localize and analyze the lesion areas without the laborious search, but also produce a medical report in a short time by a simple modification of the contents

Systems, Transfer Learning, Alternate Learning.

I. INTRODUCTION

THE medical images obtained from the Computed Tomography (CT) and the Chest X-Ray (CXR) could manifest the resulted pulmonary lesions, such as multiple ground glass opacity and infiltration. Medical imaging technologies are therefore extensively employed in coronavirus detection and contribute tremendously to the quick diagnosis of the COVID-19.

However, most medical imaging systems merely present the projections of lung condition and usually generate scans in large quantity, adding huge burdens to radiologists' workload and severely hinder the rapid diagnosis of the COVID-19. Therefore, a more intelligent system with the capacity of analyzing the lesions in images and writing corresponding medical reports automatically is of great significance to the COVID-19 diagnosis, as shown in Fig. 1.

Within such intelligent system illustrated in Fig. 1 for the COVID-19 diagnosis, medical report generation is the core component, which attempts to draw precise connections between lesion areas in images and their relevant pathological analysis in the text [1], [2]. Due to the naturally imbalanced distributions of normal and abnormal case numbers in training data, previous methods tend to focus more on the normal image patches. With the insufficient attention related to lung injuries, they usually produce undesirable findings and conclusions, which contain incorrect terminologies. Thus,

the proper import and acquisition of the external medical-specific knowledge is the key to the precise detection of the abnormal terminologies and the production of the accurate reports. Nevertheless, in previous methods, the simple application of vanilla Recurrent Neural Network (RNN) [3] and its variants [4] in language generation models without the external medical-specific knowledge hinders the model from fully utilizing the visual-and-linguistic information simultaneously.

The emergence of BERT [5] and its variant VL-BERT [6], however, provides a solution to this problem, making it possible for medical report generation system to exploit the external visual-and-linguistic knowledge simultaneously and produce more professional sentences. Equipped with this promising techniques, an efficient AI diagnosis system could be built for the quick diagnosis of the COVID-19 and largely facilitate the physicians' treatment.

However, the superior performances of deep neural network, *e.g.*, BERT and ResNet [7], usually depend on the scale of the training data. On account of the sudden outbreak of the COVID-19, the inadequate number of the training samples concerning COVID-19 becomes the main obstacle for building AI diagnosis system. Recent studies propose to introduce additional data for model training. Wang *et al.* [8] collected a set of images of viral pneumonia to expand data size. Shi *et al.* [9] added the samples of community acquired pneumonia to their COVID-19 dataset. But the model might be misguided by the introduced noisy information of other diseases and fail to capture key features of the COVID-19, resulting in poor performances on report generation.

Therefore, in this paper, to efficiently aid radiologists in diagnosis, the Medical Visual Language BERT (Medical-VLBERT) is proposed for automatic medical report generation. To effectively bridge the vision-and-language gap and improve the model performance, we further employ an alternate learning fashion that contains two procedures, which are knowledge pre-training and knowledge transferring. On one hand, the pre-training procedure learns to parse and memorize the knowledge contained in medical textbooks. On the other hand, the transferring procedure further utilize the acquired knowledge to generate medical reports. In practice, both procedures are executed on two major components: 1) *Terminology Encoder*, 2) *Shared Language Decoder*. Specifically, the *Terminology Encoder* processes the multi-modal features, *i.e.*, medical images and medical reports features, and finds their mutual relation. Then the *Shared Language Decoder* performs the sentence generation based on the information obtained from *Terminology Encoder*. For the current study on automatic medical report generation for COVID-19 cases, we are the first to construct a dataset of 368 medical findings in Chinese about 96 patients as well as 1,104 corresponding chest CT scans under the guidance of the Diagnosis and Treatment Protocol for Novel Coronavirus Pneumonia¹ Instead of combining COVID-19 data with additional information in model training, we adopt a transfer learning strategy. In practice, considering the syntactic similarity shared in medical

report, we firstly train our model on the large-scale CX-CHR dataset consisting of 45,598 X-ray images and their findings in Chinese. Then we fine tune the model on the newly-built COVID-19 datasets, using both accurate medical tags and findings on the COVID-19. Note that even though the screening techniques are different, the medical reports share the similar formats so that the transfer can benefit from the pre-trained language BERT model.

In summary, our main contributions are fourfold:

- We present Medical Visual Language BERT (Medical-VLBERT) for automatic medical report generation. It is the first model that can produce medical reports for the COVID-19 CT scans to our best knowledge.
- We adopt a transfer learning strategy in model training to alleviate the shortage of the available COVID-19 data. The transferred knowledge provides professional guidance for medical report generation. Our model achieves the state-of-the-art performances on both terminology prediction and report generation on the COVID-19 CT dataset.
- We develop an alternate training strategy for both pre-training and transferring procedures to minimize the discrepancies between the medical scans and the diagnosis texts, as well as to maximize the accuracy of the produced reports.
- We build a COVID-19 CT dataset that contains 1,104 CT scans and 368 standardized Chinese medical reports by professional radiologists based on the data of 96 patients under the guidance of the Diagnosis and Treatment Protocol for Novel Coronavirus Pneumonia. And we have released the COVID-19 CT dataset to the community².

II. RELATED WORK

A. Visual Captioning

Visual captioning [10]–[14] aims at generating a descriptive sentence for images or videos. The generated sequence is usually short, describing the main visual information in image or video in one sentence. One main stream for visual captioning method is Reinforcement learning (RL) based method, which directly uses the evaluation metrics as the reward function. The agent interacts with the environment by executing actions and receiving rewards, updating policy model parameters via gradient descent. It has gained increasing popularity in sequence generation tasks such as visual captioning [15], [16], text summarization [17], [18].

B. Medical Report Generation

Automatic generation of medical image reports is a crucial application in both academia and industry. The task is similar to image captioning. However, considering the requirements for large amounts of training data and time, the previous RL based method [1] for visual captioning is not suitable for medical report generation where the data scale is limited, especially in the recent case of the COVID-19. Many researchers have explored this area step by step, especially chest X-rays

¹The Diagnosis and Treatment Protocol for Novel Coronavirus Pneumonia (Trial Version 8): [English version](#) and [Chinese version](#).

²Website for COVID-19 CT dataset: <https://covid19ct.github.io/>

report generation [1], [19], [20]. For example, TieNet [20] classifies the chest X-rays by using both image features and text embeddings and then transformed the framework into a chest X-ray reporting system.

C. Language Model Pre-training

Learning language representations from large-scale texts in an unsupervised manner has attracted extensive attention. On one hand, ELMo [21] extracts context-sensitive word embeddings from a language model and integrates them into task-specific architectures for better feature representations. On the other hand, BERT [5] and OpenAI GPT [22] can generalize to an extensive suite of language understanding tasks without task-specific architecture designed by unsupervised pre-training. However, they are trained in general domain corpora which is quite different from the medical domain, previous pre-trained language model cannot be directly applied to accurate medical report generation.

D. Transfer Learning for Medical Diagnosis

Considering the significant differences and distributions between medical images, e.g., CT scans and X-ray, and nature images, some measures should be made to embrace the success of deep learning methods for medical diagnosis. Transfer learning [23]–[27] has the advantages of minimizing the domain gaps between different datasets and maximizing the model's capacity of generalization. Inspired by previous progress in medical image segmentation [28], lesion localization [29], stage diagnosis [30], transfer learning is leverage in our proposed model, which not only transfers the medical knowledge from textbook to the COVID-19 analysis but also addresses the issue of the shortage of the COVID-19 CT data.

E. AI-related Research against COVID-19

In spite of the rapid outbreak of the COVID-19, AI techniques can play an import role in improving and accelerating the COVID-19 diagnosis and treatment. For instance, 3-dimensional deep learning model [31] can effectively extract infection regions on CT images to increase the accuracy of the COVID-19 detection. Multi-Task Net [32] adopts a transfer learning approach to perform multi-task learning for the COVID-19 detection and segmentation on CT and X-ray scans. COVID-19-CT-CXR [33] is a public database of the COVID-19 medical images and texts, but the data is automatically extracted from the COVID-19-relevant articles and remains the issue of poor quality. Therefore, this database may not be an appropriate option of constructing an ideal AI medical diagnosis system. To the best of our knowledge, there does not exist an intelligence system for automatic medical report generation of the COVID-19.

III. METHODOLOGY

A. Overview

Our proposed model contains two key procedures: knowledge pre-training and transferring on the COVID-19 CT dataset. For knowledge pre-training, we employ a simple

lookup table to generate textbook embeddings $\mathcal{E} = \{e_i\}_{i=1}^{N_e}$, where $e_i \in R^{d_e}$. For the other procedure, we apply DenseNet-121 on CT scans to extract the spatial features $\mathcal{V} = \{v_i\}_{i=1}^{N_v}$, where the pixel-level feature vector $v_i \in R^{d_v}$. With the given textbook embeddings \mathcal{E} or the visual contexts \mathcal{V} , a Terminology Encoder is further executed to produce terminology-related features $\mathcal{M} = \{m_i\}_{i=1}^{N_m}$, where $m_i \in R^{d_m}$ represents the feature vector of a single terminology. Under the guidance of the terminology-related features \mathcal{M} , a Language Decoder is capable of generating the original textbook sequence T or the report sequence R . To bridge cross-modal gaps and achieve the semantic alignment in linguistic and visual domains, two main procedures are performed in an alternate manner via the shared Language Decoder. The overview of our proposed model is displayed in Fig. 2

B. Terminology Encoder

As shown in Fig. 3, the Terminology Encoder is built to associate the terminology representations with the visual contexts or textbook embeddings. Its architecture is the same in these two procedures except for the data inputs. In this section, the transferring procedure will be elaborated. We use the pre-defined terminology word embeddings to represent the medical domain knowledge. Then, we align each medical terminology with image regions by their coherent relation. In this manner, for each possible visual context that might imply the disease, the correlated medical terminology can be retrieved and further assisted in medical report generation.

Specifically, the Terminology Encoder is implemented on VL-BERT [6]. As a variant of BERT [5], VL-BERT encodes the input information on multi-layer bidirectional Transformer [34] and explores the hidden correlation within input elements. In the architecture of the Transformer, each input element jointly interacts with other elements by learning adaptive weights. The learned weight distributions are then transferred to the next layer. By introducing the visual inputs, VL-BERT has the ability of accommodating the linguistic and visual contents simultaneously. Therefore, VL-BERT is used to process multi-modal input pairs in our task. In the model of VL-BERT, linguistic and visual contents are processed by the attention layers, respectively. The attention layer $\text{att}(\mathbf{q}, \mathbf{k}, \mathbf{v})$ is defined as follows,

$$\begin{aligned} \text{att}(\mathbf{q}, \mathbf{k}, \mathbf{v}) &= \text{FFN}(\text{softmax}(\frac{\mathbf{q}\mathbf{k}^T}{\sqrt{d_k}})\mathbf{v}), \\ \text{FFN}(\mathbf{x}) &= \mathbf{W}_2 \cdot \max(0, \mathbf{W}_1\mathbf{x} + \mathbf{b}_1) + \mathbf{b}_2, \end{aligned} \quad (1)$$

where \mathbf{q} , \mathbf{k} and \mathbf{v} are the query, key and value vectors, respectively. d_k denotes the first dimension number of \mathbf{k} . $\text{FFN}(\cdot)$ represents the feed-forward sub-layer that contains two linear transformations and a ReLU activation, where \mathbf{W}_1 , \mathbf{W}_2 , \mathbf{b}_1 and \mathbf{b}_2 are relevant weights and biases in two linear transformations, respectively.

To jointly attend to the information from different domains in the attention layers, each terminology representation m_i needs to combine every visual feature pixel v_j to find mutual hidden relationships. Thus, we form a unified visual-

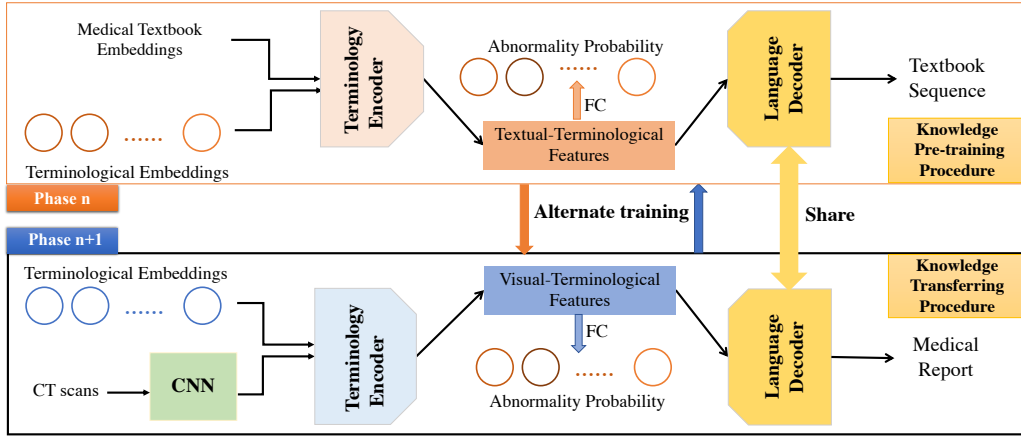


Fig. 2. The overview of our proposed Medical-VLBERT. The input images are firstly encoded as spatial features through a convolutional neural network (CNN) as the visual context. Then two separate Terminology Encoders are designed to associate the pre-defined terminology embeddings with the visual contexts and medical textbook embeddings, which produce the visual-terminological and textual-terminological features correspondingly. Besides, the alternate training strategy is exploited to minimize the discrepancies between these two terminology-related features. Based on the visual-terminological and textual-terminological features, a shared Language Decoder is employed to generate a report sequence and medical textbook sequence.

terminological features $\mathcal{P} = \{\mathbf{p}_i\}_{i=1}^{N_m+N_v}$ which is defined as follows,

$$\begin{aligned} \mathcal{P} &= \mathcal{M} \cup \mathcal{V} = \{\mathbf{p}_1, \dots, \mathbf{p}_{N_m+N_v}\} \\ &= \{\mathbf{m}_1, \dots, \mathbf{m}_{N_m}, \mathbf{v}_1, \dots, \mathbf{v}_{N_v}\}, \end{aligned} \quad (2)$$

where \cup denotes the union operation. Every element in \mathcal{P} is utilized as the input of attention layer, where self-attention and co-attention are performed simultaneously,

$$\begin{aligned} \mathbf{a}_{i*i} &= \text{att}(\mathbf{p}_i, \mathbf{p}_i, \mathbf{p}_i), \\ \mathbf{a}_{i*j} &= \text{att}(\mathbf{p}_i, \mathbf{p}_j, \mathbf{p}_i), \end{aligned} \quad (3)$$

where \mathbf{a}_{i*i} and \mathbf{a}_{i*j} denote the visual-terminological vectors after self-attention and co-attention, respectively. The processed visual-terminological features $\mathcal{A} = \{\mathbf{a}_i\}_{i=1}^{N_m+N_v}$ comprise the distributions of refined terminology-related features after the interaction between the visual features \mathcal{V} and the original terminology features \mathcal{M} . Thus they can be employed to determine which terminology is accurate to depict the signs in CT scans. The front elements of $\mathbf{a}_i \in \mathcal{A}$, $i \in [1, N_m]$ are extracted to output the updated terminology distribution.

The above formulation focuses more on the coherent relations between image regions and medical terminologies. Since the sentences in a medical report consist of a variety of terminologies, these medical terms also need to be highlighted in sentences so as to aid sentence generation. To help identify the potential relationships between medical terminologies \mathcal{M} and textbook embeddings \mathcal{E} , we also perform attention operations on these features. Similarly, we define a unified textual-terminological features $\mathcal{Q} = \{\mathbf{q}_i\}_{i=1}^{N_m+N_e}$,

$$\begin{aligned} \mathcal{Q} &= \mathcal{M} \cup \mathcal{E} = \{\mathbf{q}_1, \dots, \mathbf{q}_{N_m+N_e}\} \\ &= \{\mathbf{m}_1, \dots, \mathbf{m}_{N_m}, \mathbf{e}_1, \dots, \mathbf{e}_{N_e}\}. \end{aligned} \quad (4)$$

Following that, the textual-terminological features \mathcal{Q} are sent to the attention layer for further coherent relationship exploration,

$$\begin{aligned} \mathbf{t}_{i*i} &= \text{att}(\mathbf{q}_i, \mathbf{q}_i, \mathbf{q}_i), \\ \mathbf{t}_{i*j} &= \text{att}(\mathbf{q}_i, \mathbf{q}_j, \mathbf{q}_i), \end{aligned} \quad (5)$$

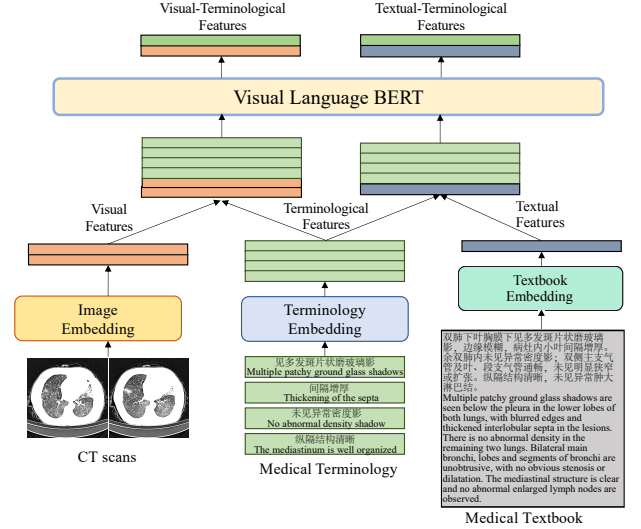


Fig. 3. The illustration of the Terminology Encoder. Terminology Encoder is implemented in Visual Language BERT (VLBERT). Terminology embeddings are grouped with visual and textual embeddings, respectively, to form parallel corresponding inputs for visual language BERT.

where \mathbf{t}_{i*i} and \mathbf{t}_{i*j} denote the textual-terminological vectors after self-attention and co-attention, respectively. The obtained textual-terminological features $\mathcal{T} = \{\mathbf{t}_i\}_{i=1}^{N_m+N_e}$ can be utilized for sentence generation, since they contain the corresponding information between text embeddings \mathcal{E} and medical terminologies \mathcal{M} . More specifically, they act like a grammar book that can provide references and norms for medical terminologies to generate a professional sentences. For example, medical terminology “pulmonary vascularity” could be utilized to generate a simple sentence like “Pulmonary vascularity is within normal limits”, since \mathcal{T} contains a connection between “spine” and “there are minimal degenerative changes of the spine”. The front elements of $\mathbf{t}_i \in \mathcal{T}$, $i \in [1, N_m]$ can also be exploited to scrutinize the acquired terminology distribution.

The acquired terminology distribution from textual-

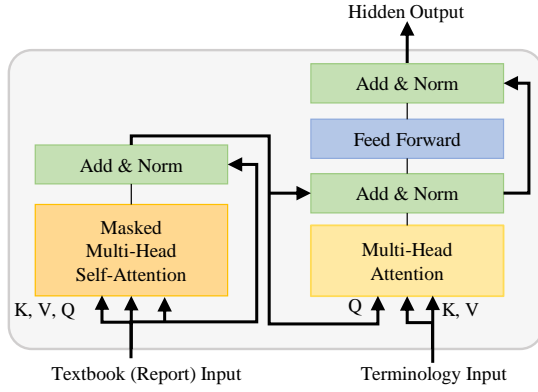


Fig. 4. The illustration of a **block** in Language Decoder. Terminology Input denotes terminology-related features *i.e.*, Visual-Terminological features or Textual-Terminological features, from Terminology Encoder. Text (Report) Input denotes word embeddings from textbook or report.

terminological features or visual-terminological features is used for abnormality classification. We treat the abnormality classification as a multi-label classification task and predict scores as follows,

$$x_i = \text{sigmoid}(\mathbf{W}_{\hat{\mathbf{m}}}\hat{\mathbf{m}}_i + \mathbf{b}_{\hat{\mathbf{m}}}),$$

$$\mathcal{L}_{cls} = \frac{1}{N_m} \sum_{i=1}^{N_m} [y_i \log x_i + (1 - y_i) \log (1 - x_i)], \quad (6)$$

where $\hat{\mathbf{m}}_i \in \mathcal{A}$ or \mathcal{T} , $i \in [1, N_m]$, $\mathbf{W}_{\hat{\mathbf{m}}}$ and $\mathbf{b}_{\hat{\mathbf{m}}}$ are parameters of a linear projection, respectively. This projection transforms terminology-related features into a distribution over all terminologies. \mathcal{L}_{cls} is the average binary cross entropy loss, x_i denotes probability of abnormal medical term $\hat{\mathbf{m}}_i$, y_i is the ground truth label and N_m is the number of abnormalities, that is the number of medical terminologies.

C. Shared Language Decoder

We design a shared Language Decoder to perform alternate training and enable the semantic alignment in linguistic and visual domains.

Given a set of medical textbook or report tokens $\mathcal{R} = \{\mathbf{r}_i\}_{i=1}^{N_r}$, we adopt a standard language modeling objective [22] to maximize the likelihood in the following formulation:

$$P(\mathbf{r}_1, \mathbf{r}_2, \dots, \mathbf{r}_{N_r}; \Theta_{\mathcal{R}}) = \prod_{i=1}^{N_r} P(\mathbf{r}_i | \mathbf{r}_1, \mathbf{r}_2, \dots, \mathbf{r}_{i-1}; \Theta_{\{\mathbf{r}_j\}_{j=1}^{i-1}}),$$

$$\mathcal{L}(\mathcal{R}) = - \sum_{i=1}^{N_r} \log P(\mathbf{r}_i | \mathbf{r}_1, \dots, \mathbf{r}_{i-1}; \Theta_{\mathcal{R}}), \quad (7)$$

where $P(\mathbf{r}_i | \mathbf{r}_1, \mathbf{r}_2, \dots, \mathbf{r}_{i-1}; \Theta_{\{\mathbf{r}_j\}_{j=1}^{i-1}})$ is the probability of next token conditioned in the history sequence and parameters $\Theta_{\{\mathbf{r}_j\}_{j=1}^{i-1}}$, and $\mathcal{L}(\mathcal{R})$ denotes the corresponding loss in text generation.

Based on the history sequence $\{\mathbf{r}_1, \dots, \mathbf{r}_{i-1}\}$, our shared Language Decoder applies a multi-head attention operation over the medical terminology-related features, *i.e.*, Visual-Terminological features or Textual-Terminological features,

followed by position-wise feed-forward networks to compute a probability distribution $P(i)$ over tokens in the vocabulary,

$$h_0 = \mathbf{w}E_{\mathbf{w}} + \mathbf{p}E_{\mathbf{p}},$$

$$\mathbf{h}_l = \mathbf{block}(\mathbf{h}_{l-1}, \hat{\mathbf{m}}) \quad \forall l \in [1, N], \quad (8)$$

$$P(i) = \text{softmax}(\mathbf{h}_N E_{\mathbf{w}}^T),$$

where \mathbf{w} is the vocabulary index vector, \mathbf{p} is the position index vector, $E_{\mathbf{w}}$ is the word embedding matrix, $E_{\mathbf{p}}$ is the position embedding matrix the index vector of position, and **block** is the architecture of Transformer decoder block, which is depicted in Fig. 4.

D. Alternate Training Strategy

In terms of data distribution and input source information (language or vision), there exists a large semantic deviation between the collected medical textbooks and image report datasets. Unlike recent language representation models [5], [22] which are trained in an unsupervised manner, we develop a strategy in Algorithm 1 to alleviate data bias and narrow the gap between language and vision domains.

Algorithm 1 Alternate Training Strategy

- 1: Initialize the shared Language Decoder (\mathcal{D});
- 2: **repeat**
- 3: Load \mathcal{D} and execute the pre-training procedure;
- 4: Optimize \mathcal{D} ;
- 5: Stop the pre-training procedure;
- 6: Load \mathcal{D} and execute the transferring procedure;
- 7: Optimize \mathcal{D} .
- 8: Stop the transferring procedure;
- 9: **until** Convergence

In each epoch, we train the shared Language Decoder with Terminology Encoder in an end-to-end manner to optimize the objective function discussed in Eq. 9. Specifically, the knowledge pre-training procedure is firstly executed for the first epoch to optimize the decoder. In the next epoch, the pre-training procedure is halted and the transferring procedure is started to fine-tune the trained decoder. Finally, the trained decoder is re-loaded in the pre-training procedure, and the above operation is repeated until convergence. With the alternate training strategy, these two procedures can exchange knowledge and adapt mutually.

E. Optimization

Training samples consist of tuples $(\mathbf{y}, \mathcal{T})$ or triplets $(I, \mathbf{y}, \mathcal{T})$ in pre-training or transferring procedure respectively, where I is an image, \mathbf{y} denotes the ground-truth abnormalities and \mathcal{T} is the original textbook sequence or ground-truth report. Formally, we define a multi-task loss as follows:

$$\mathcal{L} = \lambda \mathcal{L}_{cls} + \mathcal{L}_{\mathcal{T}}, \quad (9)$$

where \mathcal{L}_{cls} is the terminology multi-label classification loss defined in Eq. 6, $\mathcal{L}_{\mathcal{T}}$ is token-level cross entropy loss defined in Eq. 7, and $\lambda = 1$ is a balance weight. The encoder-decoder architecture is jointly trained to minimize \mathcal{L} .

IV. EXPERIMENTS

A. Dataset

Two medical image datasets are employed to evaluate the performance of our proposed Medical-VLBERT.

COVID-19 CT The COVID-19 CT dataset is a collection of the chest CT images with Chinese reports for the COVID-19 checking, consisting of 368 medical reports and 1,104 CT images from 96 patients. We count the details of these patients and the distribution of ages, counts of samples in age range and the gender percentages are shown in the Fig. 5. In the raw data, each report accompanies a set of CT images. We filter 10 CT images characterizing distinct features for each report and build our own COVID-19 CT dataset for report generation.

CX-CHR CX-CHR is a **large-scale** collection of chest X-ray images with Chinese reports for health checking, consisting of 45,598 images of 35,609 patients and 28,299 medical image-report pairs. In addition, CX-CHR includes 12 million external medical textbooks from a Chinese medical website³, which contains symptoms, manifestations, laboratory tests and other information on various diseases in thoracic surgery.

B. Implementation Details

We implement our method on Pytorch Framework and conduct the training on two GPUs. **DenseNet-121** [35] is adopted as the backbone, which takes a 224×224 CT image as input to achieve (7, 7, 1024) feature maps from the last convolution layer. The dimension of all liner projection layers is set to 512. To balance language model perplexity with model size and computational requirements, we set the embedding and the hidden size of both **VLBERT** and Language Decoder to 512. The numbers of hidden layers and attention heads of Terminology Encoder are of 2 and 8 respectively. Due to the better performance achieved by concatenation than summation in practice, we adopt concatenation as the feature fusion approach. To minimize the loss function, we employ the same ADAM optimizer in training with a batch size of 32. The backbone is trained with a learning rate of 10^{-6} and the two knowledge procedures are trained with a learning rate of 5×10^{-5} for 30 epochs. At the beginning, we train the model on the large-scale CX-CHR dataset by Alternate Training Strategy. Then we fine tune the model on our COVID-19 CT dataset with the Alternate Training Strategy as well. Due to the scale of the COVID-19 CT dataset, we enhance the transferring procedure, which means that we execute the pre-training procedure once and the transferring procedure multiple times at one epoch.

C. Evaluation metrics

The evaluation of our experiments consists of objective automatic evaluation and subjective human evaluation. To provide fair and clear evaluation results of our model, different metrics are employed for such two types of evaluations.

Objective Evaluation The evaluation metrics for objective automatic evaluation contain BLEU (uni-gram to 4-gram), ROUGE-L, and CIDEr-D. BLEU [36] is a classic algorithm

for automatic evaluation of machine translation. It measures the consensus between the machines' output and the human being's output and is thus applied to test the accuracy of generated reports. ROUGE-L [37] is another most-used metric in machine translation. On the basis of the longest common sub-sequence statistics, ROUGE-L computes the correlation between a candidate translation and other references. So it is suitable to measure the correspondence between the produced sentences and the original expressions. CIDEr-D [38] is a specialized metric for image captioning evaluation that measures the similarities between image descriptions and the reference sentences. Therefore it is used in our evaluation of the text generation based on the COVID-19 CT scans.

Subjective Evaluation To give more convincing performances of our presented model, we further conduct subjective human evaluation by radiologists following HRGR-Agent [1]. We randomly select 16 CT scans of the COVID-19 patients and the corresponding reports generated by Medical-VLBERT, DenseNet+GPT-2 and professional radiologists. Here, Medical-VLBERT is our proposed model and DenseNet+GPT-2 is the model using GPT-2 [39] as terminology encoder and using the Alternate Training Strategy. Three native Chinese radiologists are invited to view three reports and provide rankings to sort out which is the best produced report. Specifically, the best report is categorized as 1, the second best one is categorized as 2, and the worst one is classified as 3. Then we count the sum of categories of 1, 2, and 3 for three reports, respectively.

TABLE I
ARCHITECTURES OF COMPARED METHODS. CE IS SHORT FOR CROSS-ENTROPY. RL DENOTES THE DECODER OPTIMIZED BY REINFORCEMENT LEARNING. TEMPLATE DENOTES THE DECODER GENERATING SENTENCES FROM A TEMPLATE DATABASE.

Models	Encoder	Decoder	Strategy
CoAtt [2]	CNN	RNN	CE
HRGR-Agent [1]	CNN	RNN+Template	CE+RL
KERP [19]	CNN+Attention	Template	CE
Vision-BERT [5]	CNN	Pre-trained Decoder	CE
DenseNet+GPT-2	Transformer Encoder	Pre-trained Decoder	CE+Alternate
Medical-VLBERT	VLBERT	Pre-trained Decoder	CE+Alternate

D. Quantitative Results

CX-CHR As shown in Table I, we compare our proposed model with other medical report generation methods. Table II shows the performance of these models on the CX-CHR dataset. The results across automatic evaluation metrics consistently indicate that by exploiting the medical-specific knowledge recorded in large-scale unlabeled medical textbooks, the proposed Medical-VLBERT achieves superior performance than all the state-of-the-art techniques [1], [19].

Furthermore, to verify the capability of the language-to-vision transfer, Medical-VLBERT is compared with Vision-BERT [5] by combining our Terminology Encoder and BERT model. As shown in the fourth row of Table II, our model outperforms other models significantly: it improves KERP on CIDEr-D by 37.0%, ROUGE-L by 3.7%, BLEU-1 by 2.7%, BLEU-2 by 3.9%, BLEU-3 by 3.8% and BLEU-4 by 6.1%. And comparing with DenseNet + GPT-2, as shown in the fifth row in Table II, our Terminology Encoder performs better.

³<http://www.fh21.com.cn>

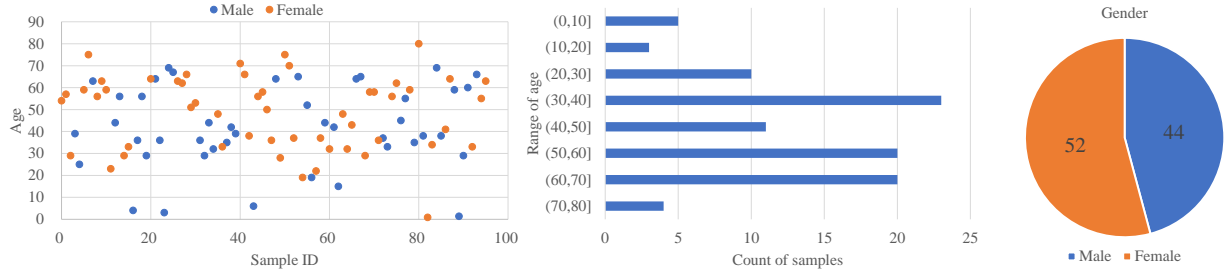


Fig. 5. The age and gender distribution of the COVID-19 patients in our COVID-19 CT dataset. The range of age is from 10 months old to 80 years old.

TABLE II
PERFORMANCE COMPARISON ON THE LARGE SCALE CX-CHR DATASET.

Models	CIDEr-D	ROUGE-L	BLEU@1	BLEU@2	BLEU@3	BLEU@4
CoAtt [2]	273.5	64.5	64.7	57.5	52.5	48.7
HRGR-Agent [1]	289.5	61.2	67.3	58.7	53.0	48.6
KERP [19]	285.0	61.8	67.3	58.8	53.2	47.3
Vision-BERT [5]	302.4	63.7	68.6	60.1	54.1	50.3
DenseNet + GPT-2	317.7	64.6	68.8	60.7	55.7	52.1
Medical-VLBERT (Ours)	322.0	65.5	70.0	62.7	57.0	53.4

CT Scan	Ground Truth	Medical-VLBERT	DenseNet + GPT-2
	<p>双肺多发磨玻璃密度斑片及大片影，以胸膜下为著；双侧主支气管及叶、段支气管通畅，未见明显狭窄或扩张。纵隔结构清晰，未见异常肿大淋巴结。双侧胸膜未见增厚，双侧胸腔未见积液。</p> <p>Multiple ground glass density patches and large shadows are seen in both lungs, mainly in the subpleural area; Bilateral main bronchi, lobes and segments of bronchi are unobtrusive, with no obvious stenosis or dilatation. The mediastinal structure is clear and no abnormal enlarged lymph nodes are observed. There is no thickening of bilateral pleura and no effusion in bilateral pleura.</p>	<p>双肺多发磨玻璃密度斑片及大片影，以胸膜下为著，下肺为重；双侧主支气管及叶、段支气管通畅，未见明显狭窄或扩张。纵隔结构清晰，未见异常肿大淋巴结。双侧胸膜未见增厚，双侧胸腔未见积液。</p> <p><u>Multiple ground glass density patches and large shadows are seen in both lungs, mainly in the subpleural area and the lower lung. Bilateral main bronchi, lobes and segments of bronchi are unobtrusive, with no obvious stenosis or dilatation. The mediastinal structure is clear and no abnormal enlarged lymph nodes are observed. There is no thickening of bilateral pleura and no effusion in bilateral pleura.</u></p>	<p>双肺散在多发磨玻璃密度斑片，边界稍模糊，以为明显；双肺下叶少许纤维灶。双侧主支气管及叶、段支气管通畅，未见明显狭窄或扩张。纵隔结构清晰，未见异常肿大淋巴结。双侧胸膜未见增厚，双侧胸腔未见积液。</p> <p>Double lungs scatter in multiple ground glass density patches, slightly blurred boundary, thought to be obvious; A few fibrous foci are in the lower lobes of both lungs. Bilateral main bronchi, lobes and segments of bronchi are unobtrusive, with no obvious stenosis or dilatation. The mediastinal structure is clear and no abnormal enlarged lymph nodes are observed. There is no thickening of bilateral pleura and no effusion in bilateral pleura.</p>
	<p>双肺多发磨玻璃密度斑片及大片影，以胸膜下为著，下肺为重；双侧主支气管及叶、段支气管通畅，未见明显狭窄或扩张。纵隔结构清晰，未见异常肿大淋巴结。双侧胸膜未见增厚，双侧胸腔未见积液。</p> <p>Multiple ground glass density patches and large shadows are seen in both lungs, mainly in the subpleural area and the lower lung. Bilateral main bronchi, lobes and segments of bronchi are unobtrusive, with no obvious stenosis or dilatation. The mediastinal structure is clear and no abnormal enlarged lymph nodes are observed. There is no thickening of bilateral pleura and no effusion in bilateral pleura.</p>	<p>双肺散在多发斑片状模糊影，分布以胸膜下为主，可见部分实变；双肺下叶见少许条索影；双侧主支气管及叶、段支气管通畅，未见明显狭窄或扩张。纵隔结构清晰，未见异常肿大淋巴结。双侧胸膜未见增厚，双侧胸腔未见积液。肝脏密度均匀减低。</p> <p>Multiple patchy fuzzy shadows are scattered in both lungs, mainly distribute under the pleura, and some consolidation is visible. A few filaments are seen in the lower lobe of both lungs. Bilateral main bronchi, lobes and segments of bronchi are unobtrusive, with no obvious stenosis or dilatation. The mediastinal structure is clear and no abnormal enlarged lymph nodes are observed. There is no thickening of bilateral pleura and no effusion in bilateral pleura. The liver density decreased uniformly.</p>	<p>双肺散在多发磨玻璃密度影及边缘模糊小结节，局部病灶较前缩小，密度较前浅淡；双肺散在实性小结节；双肺内未见异常密度影；双侧主支气管及叶、段支气管通畅，未见明显狭窄或扩张。纵隔结构清晰，未见异常肿大淋巴结。双侧胸膜未见增厚，双侧胸腔未见积液。主动脉见钙化斑，胸椎骨质增生。肝脏多发囊状低密度影。</p> <p>Double lungs scatter in multiple ground glass density shadow and the edge of the fuzzy nodules, local lesions are smaller than before, the density is lighter than before; Scattered solid nodules of double lungs; No abnormal density shadow is found in both lungs. Bilateral main bronchi, lobes and segments of bronchi are unobtrusive, with no obvious stenosis or dilatation. The mediastinal structure is clear and no abnormal enlarged lymph nodes are observed. There is no thickening of bilateral pleura and no effusion in bilateral pleura. Calcified plaques are seen in the aorta and hyperosteoecy of the thoracic vertebra. Multiple cystic low density shadows in the liver.</p>

Fig. 6. Illustrations of the reports generated by Medical-VLBERT and DenseNet+GPT-2. The underlined sentences are the descriptions of lesions that match the original ones in the ground truth. The selected CT scans are from the test dataset.

COVID-19 CT After training on the CX-CHR dataset, we use the pre-trained model and fine tune on the COVID-19 CT dataset. In order to compare with our Medical-VLBERT, we adopt DenseNet+GPT-2 as the baseline, where DenseNet [35] encodes CT image, Transformer [34] encoder acts as Terminology Encoder, and GPT-2 acts as the Language Decoder. Due to the small scale of the COVID-19 data, we conduct different experiments with different Alternate Training Strategies. As the results shown in Table III, a proper strategy is very

important for our Medical-VLBERT and it could boost around 100% in CIDEr-D score. But for baseline, more Transferring Procedures in one epoch could only improve BLEU score, and even decrease CIDEr-D and ROUGE-L score. As default, we will execute 1 time Pre-Training Procedure and 3 times Transferring Procedure in one epoch in other experiments.

Then we explore the impact of the number of hidden layers of Medical-VLBERT. As shown in Table IV, we adopt CoAtt [2], Vision-BERT [5] and VGG+GPT-2 and DenseNet+GPT-2 as the baselines. Two hidden layers perform

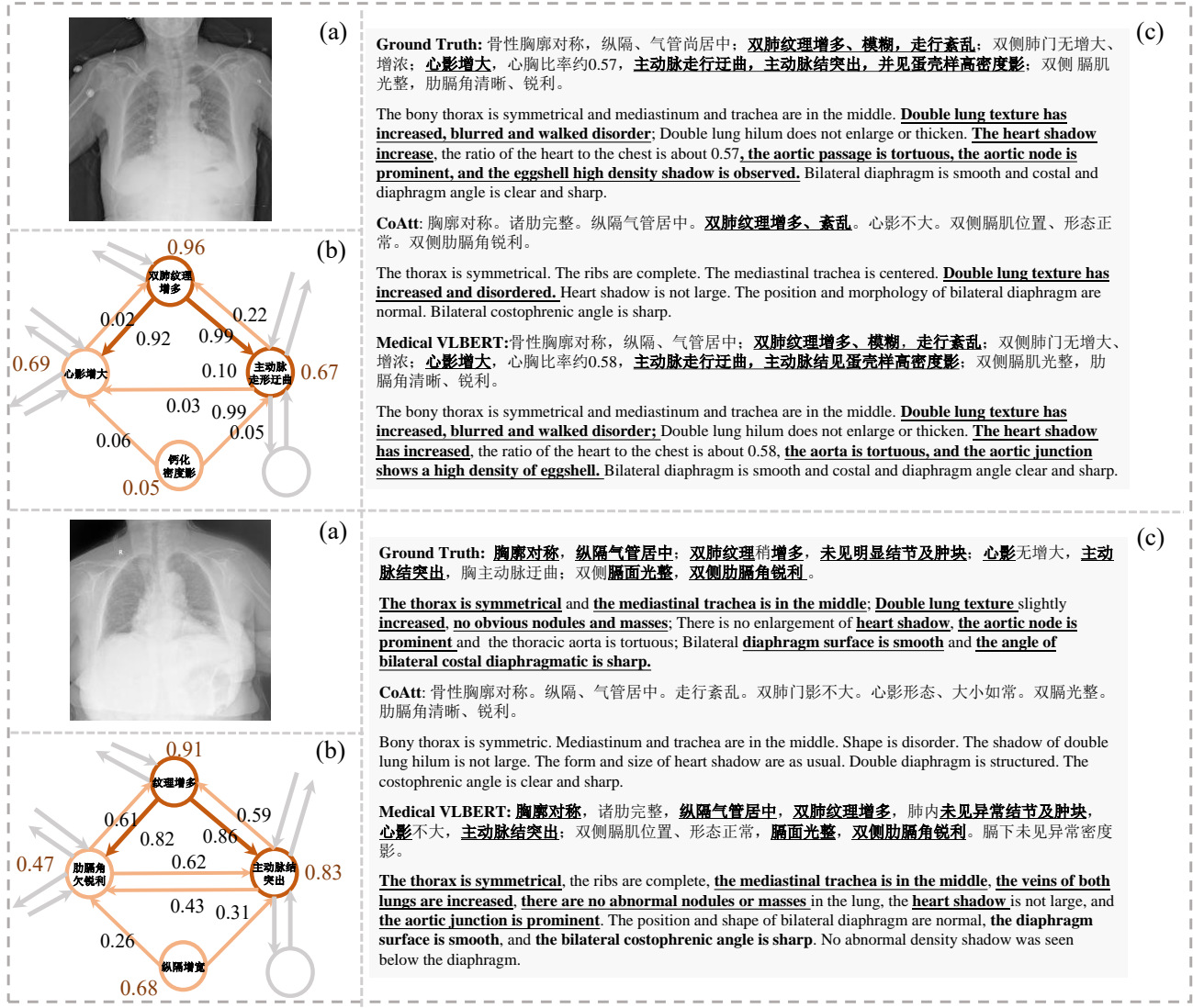


Fig. 7. Visualization of the results generated by CoAtt [2] and Medical-VLBERT on the CX-CHR dataset. (b) The orange digits represent classification scores, and black digits denote attention weights; (c) The underlined texts represent the alignment between generated and ground truth reports.

the best results in all metrics. As the number of hidden layers increases, the parameters increase as well. Though the expression ability of the model is larger, it will converge slowly and require more independent data.

As mentioned before, there is also an abnormality classification module in our model. As shown in Table V, we adopt DenseNet, Resnet and VGG as the baselines to do the multi-label classification directly. We can see our model outperforms the baselines, which means the Terminology Encoder can reinforce the feature extraction of abnormalities.

E. Visualization Results

The medical reports generated by our Medical-VLBERT, DenseNet+GPT-2 and professional radiologists (ground truth) are show in Fig. 6. Note that Medical-VLBERT produces paragraphs of CT scans which is more similar to that of professional radiologists than DenseNet+GPT-2. More specifically, Medical-VLBERT has the advantage of generating

more accurate medical terminologies as well as more concise descriptions. By comparison, DenseNet+GPT-2 seemingly learns to provide a long-winded report template but has fewer matched medical terminologies.

The visualized results on the CX-CHR dataset are provided in Fig. 7. The generated reports demonstrate the significant alignment with ground truth reports. Furthermore, the sub-figures (b) illustrate how knowledge of textbooks influences the generated reports.

Fig. 8 provides the visualization of activation mapping of our model on the COVID-19 CT dataset. The maps demonstrate the alignment with the lesion areas. During the inference, radiologists can judge the correctness of the generated report by checking the activation maps.

The attention maps of three textbooks are presented in Fig. 9. The dark patches demonstrate that the knowledge pre-training procedure helps learn medical-specific and terminology-related knowledge contained in the medical textbooks. The knowledge transferring procedure helps transfer

TABLE III
PERFORMANCE COMPARISON ON DIFFERENT ALTERNATE TRAINING STRATEGY. (m,n) MEANS THAT EXECUTE m TIMES PRE-TRAINING PROCEDURE AND n TIMES TRANSFERRING PROCEDURE AT ONE EPOCH.

Models	Strategy	CIDEr-D	ROUGE-L	BLEU@1	BLEU@2	BLEU@3	BLEU@4
DenseNet + GPT-2	(1,1)	23.2	58.9	32.1	31.0	30.3	29.7
	(1,3)	23.1	51.4	55.3	47.6	42.3	39.0
	(1,4)	17.7	51.5	51.5	44.4	40.4	37.7
	(1,5)	15.6	52.9	56.6	48.3	43.4	40.3
Medical-VLBERT (Ours)	(1,1)	20.7	51.6	55.6	47.3	42.8	39.6
	(1,3)	115.8	59.1	61.8	55.1	51.0	48.4
	(1,4)	122.8	59.6	61.6	55.6	51.9	49.4
	(1,5)	117.4	60.3	63.4	57.2	53.6	51.3

TABLE IV
PERFORMANCE COMPARISON ON OUR COVID-19 CT DATASET. MEDICAL-VLBERT@ N IS SHORT FOR MEDICAL-VLBERT WITH N HIDDEN LAYERS.

Models	CIDEr-D	ROUGE-L	BLEU@1	BLEU@2	BLEU@3	BLEU@4
CoAtt [2]	25.5	57.4	60.8	53.5	49.4	46.8
Vision-BERT [5]	29.6	57.8	57.9	51.4	47.5	44.9
DenseNet + GPT-2	23.1	51.4	55.3	47.6	42.3	39.0
VGG + GPT-2	31.5	51.3	55.8	48.0	42.6	39.2
Medical-VLBERT@6	76.6	57.2	59.3	52.5	48.5	25.9
Medical-VLBERT@4	97.6	57.5	59.4	52.9	49.0	46.5
Medical-VLBERT@2	115.8	59.1	61.8	55.1	51.1	48.4

TABLE V
RESULTS OF TAG CLASSIFICATION

Models	Precision(%)	Recall(%)	F1(%)
CoAtt [2]	16.2	66.7	19.9
Densenet [35]	21.4	21.6	20.9
Resnet [7]	42.8	26.8	28.9
VGG [40]	23.4	20.9	20.0
Medical-VLBERT	64.7	49.0	52.3

the knowledge and bridge the gap between language and vision for report generation. Therefore, our proposed Medical-VLBERT can provide a more satisfactory report for the COVID-19 diagnosis in practice.

F. Subjective Evaluation by Radiologists

We make a summary of the subjective evaluation by radiologists in Fig. 10. It is evident that report obtained by our proposed Medical-VLBERT receives the second most votes as the best report (Category 1), merely fewer votes than that of humans, i.e., ground-truth reports, by 6. Medical-VLBERT's report also has better evaluation than DenseNet+GPT-2's one, since the report generated by DenseNet+GPT-2 is mostly voted as the worst report (Category 2). The results in Fig. 10 can well demonstrate that Medical-VLBERT has excellent performance in report generation and produce medical texts more similar to that of humans.

G. Ablation Studies

To verify the most important components of our proposed Medical-VLBERT model, we conduct the ablation studies via replacing or removing specific components within our model. All results of ablation studies are displayed in Table VI.

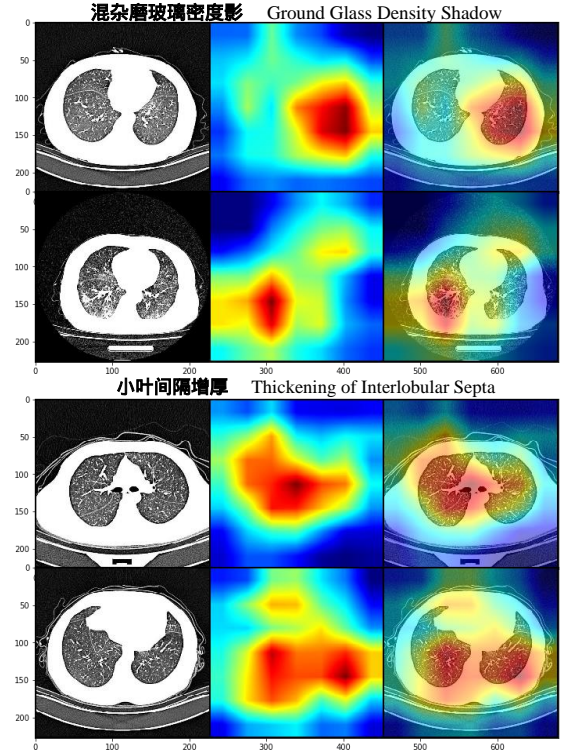


Fig. 8. Visualization of the activation mapping generated by Medical-VLBERT on the COVID-19 CT dataset. The patterns of “Ground Glass Density Shadow” and “Thickening of Interlobular Septa” denote the existence of some ground glass shadows and lots of fine and linear white shadows, respectively.

External Knowledge External medical knowledge plays a significant role in our model training. The introduction of external knowledge by pre-training the Language Decoder in the medical domain corpus further boosts the model's

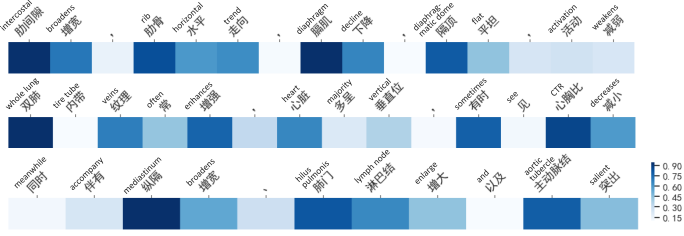


Fig. 9. The attention maps of three textbooks indicate what knowledge the pre-training procedure has acquired.

Subjective Evaluation by Radiologists

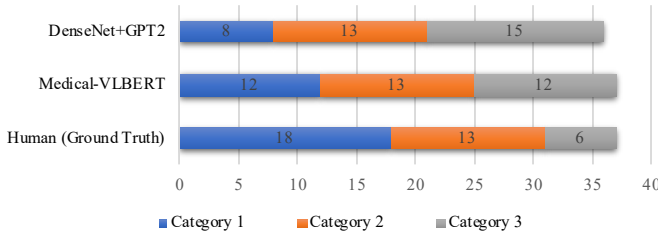


Fig. 10. Subjective evaluation by three radiologists on the reports generated by Medical-VLBERT, DenseNet+GPT-2 and humans, where the best report is categorized as 1, the second best as 2, and the worst as 3.

performance. According to the results of the first and third row in Table VI, BLEU increase significantly, but CIDEr-D and ROUGE-L decrease. Owing to the small scale of the COVID-19 CT dataset, the model tends to overfit without external knowledge. As a result, the model is prone to produce more words from training set, leading to high ROUGE-L. However, if we introduce the EK into the model, it would learn more general medical knowledge and generate fewer unrelated words, resulting in a high BLEU. Moreover, CIDEr-D assigns low weight to high-frequency phrases, but there are many keywords with high frequency in the dataset for medical report generation. According to the results of the second and fourth row in the Table VI, the addition of the EK only increases CIDEr-D. However, as presented in the last four rows in Table VI, the addition of the EK to the model with the ATS boosts the performances on all the metrics, which demonstrates that the strategy of introducing external knowledge is useful.

Alternate Training We design an experiment to validate its effectiveness of the alternate training strategy on the condition that external knowledge exists. The Medical-VLBERT is first trained on collected medical textbooks and then trained on CT images for 30 epochs, which means that knowledge pre-training and transferring procedures are separately executed. As expected, experimental results in the last four rows in Table VI show that our model's performance is weakened without alternate training. Due to the lack of efficient knowledge transferring, the shared Language Decoder are easily affected by data bias and domain misalignment between language and vision. Thus, the model is unable to effectively make use of the linguistic knowledge in medical text and, as a result, generate unsatisfactory paragraphs. Therefore, alternate

TABLE VI
PERFORMANCE CONTRIBUTION OF EACH COMPONENT IN MEDICAL-VLBERT ON THE COVID-19 CT. ATS, TLS AND EK ARE SHORT FOR ALTERNATE TRAINING STRATEGY, TRANSFER LEARNING STRATEGY AND EXTERNAL KNOWLEDGE.

Components			Evaluation Metrics			
ATS	TLS	EK	CIDEr-D	ROUGE-L	BLEU@-1	BLEU@-4
-	-	-	110.2	60.6	47.9	39.9
-	✓	-	28.5 ^{↓81.7}	56.3 ^{↓4.3}	57.5 ^{↑9.6}	44.2 ^{↑4.3}
-	-	✓	40.6 ^{↓69.6}	55.7 ^{↓4.9}	58.7 ^{↑10.8}	45.1 ^{↑5.2}
-	✓	✓	38.3 ^{↓71.9}	55.9 ^{↓4.7}	56.0 ^{↑8.1}	42.6 ^{↑2.7}
✓	-	✓	95.7 ^{↓14.5}	59.0 ^{↓1.6}	59.0 ^{↑11.1}	46.6 ^{↑6.7}
✓	✓	✓	115.8 ^{↑5.6}	59.1 ^{↓1.5}	61.8 ^{↑13.9}	48.4 ^{↑8.5}

training strategy enables two procedures to adapt mutually and that the shared Language Decoder of model receive better optimization.

Transfer Learning We adopt a transfer Learning strategy to alleviate the shortage of the available COVID-19 data. We conduct experiments to verify whether model has better performance after transferring from the large-scale CX-CHR dataset. As shown in Table VI, the results of the first and second row on CIDEr-D and BLEU prove that the model is able to exploit the knowledge from the CX-CHR dataset and improve the performance on the COVID-19 dataset. As the results of the third and fourth row shown in Table VI, the TLS cannot provide improvement to the model without the ATS. Nevertheless, as the fifth and sixth row displayed in Table VI, the addition of the TLS gives better results with the ATS, which implies the ATS could enhance the advantage of TLS.

V. CONCLUSION

In this work, we proposed the Medical Visual Language BERT (Medical-VLBERT) model for automatic medical report generation on the COVID-19 CT scans. Medical-VLBERT further adopts an alternate learning strategy that can use the transferred medical textual knowledge to identify the abnormality in CT images and generate the medical report automatically based on the detected lesion regions with acquired knowledge. Besides, we built a COVID-19 CT dataset of 368 medical findings in Chinese and 1,104 chest CT scans from the first affiliated hospital of Jinan University Guangzhou and fifth affiliated hospital of Sun Yat-sen University Zhuhai in China. To solve the COVID-19 data shortage problem, we employed a transfer learning fashion in which the model are firstly trained on the large-scale CX-CHR dataset in Chinese, and then fine-tuned on the COVID-19 CT dataset. Results and analysis in our experiments proved that our model has state-of-the-art performances on terminology prediction and report generation on the Chinese COVID-19 CT dataset and Chinese CX-CHR dataset. Furthermore, in clinical practice, our model could help ease the radiologists' burdens via aiding their diagnostic workflow, including analyzing the lesions in images and writing corresponding medical reports for diagnosed patients. In the future, we will pay more attention to the diagnostic phase information on a patient's timelines and focus on the generation of more integrated reports.

ACKNOWLEDGMENT

The work was supported in part by Key Area R&D Program of Guangdong Province with grant No. 2020B0101350001, Key Area R&D Program of Guangdong Province with grant No.2018B030338001, by the National Key R&D Program of China with grant No.2018YFB1800800, by Shenzhen Outstanding Talents Training Fund, by Guangdong Research Project No.2017ZT07X152, by NSFC-Youth 61902335, by Guangdong Regional Joint Fund-Key Projects 2019B1515120039, by The National Natural Science Foundation Fund of China (61931024), by helixon biotechnology company Fund and CCF-Tencent Open Fund.

REFERENCES

- [1] C. Y. Li, X. Liang, Z. Hu, and E. P. Xing, "Hybrid retrieval-generation reinforced agent for medical image report generation," in *NeurIPS*, 2018.
- [2] B. Jing, P. Xie, and E. Xing, "On the automatic generation of medical imaging reports," in *ACL*, 2018.
- [3] L. Jing *et al.*, "Gated orthogonal recurrent units: On learning to forget," *Neural Computation*, vol. 31, no. 4, pp. 765–783, 2019.
- [4] A. Karpathy and L. Fei-Fei, "Deep visual-semantic alignments for generating image descriptions," in *CVPR*, 2015.
- [5] J. Devlin, M.-W. Chang, K. Lee, and K. Toutanova, "Bert: Pre-training of deep bidirectional transformers for language understanding," in *NAACL-HLT*, 2018.
- [6] W. Su *et al.*, "VL-BERT: Pre-training of generic visual-linguistic representations," in *ICLR*, 2020.
- [7] K. He, X. Zhang, S. Ren, and J. Sun, "Deep residual learning for image recognition," in *CVPR*, 2016, pp. 770–778.
- [8] S. Wang, B. Kang, J. Ma, X. Zeng, M. Xiao, J. Guo, M. Cai, J. Yang, Y. Li, X. Meng *et al.*, "A deep learning algorithm using ct images to screen for corona virus disease (covid-19)," *European radiology*, vol. 31, no. 8, pp. 6096–6104, 2021.
- [9] F. Shi *et al.*, "Large-scale screening of covid-19 from community acquired pneumonia using infection size-aware classification," *arXiv preprint arXiv:2003.09860*, 2020.
- [10] J. Krause, J. Johnson, R. Krishna, and L. Fei-Fei, "A hierarchical approach for generating descriptive image paragraphs," in *CVPR*, 2017.
- [11] P. Anderson *et al.*, "Bottom-up and top-down attention for image captioning and visual question answering," in *CVPR*, 2018.
- [12] O. Vinyals, A. Toshev, S. Bengio, and D. Erhan, "Show and tell: A neural image caption generator," in *CVPR*, 2015.
- [13] K. Xu *et al.*, "Show, attend and tell: Neural image caption generation with visual attention," in *ICML*, 2015.
- [14] T. Yao, Y. Pan, Y. Li, and T. Mei, "Exploring visual relationship for image captioning," in *ECCV*, 2018.
- [15] S. J. Rennie, E. Marcheret, Y. Mroueh, J. Ross, and V. Goel, "Self-critical sequence training for image captioning," in *CVPR*, 2017.
- [16] S. Liu, Z. Zhu, N. Ye, S. Guadarrama, and K. Murphy, "Improved image captioning via policy gradient optimization of spider," in *ICCV*, 2017.
- [17] X. Wang, W. Chen, Y.-F. Wang, and W. Y. Wang, "No metrics are perfect: Adversarial reward learning for visual storytelling," in *ACL*, 2018.
- [18] L. Wang, J. Yao, Y. Tao, L. Zhong, W. Liu, and Q. Du, "A reinforced topic-aware convolutional sequence-to-sequence model for abstractive text summarization," in *IJCAI*, 2018.
- [19] C. Y. Li, X. Liang, Z. Hu, and E. P. Xing, "Knowledge-driven encode, retrieve, paraphrase for medical image report generation," in *AAAI*, 2019.
- [20] X. Wang, Y. Peng, L. Lu, Z. Lu, and R. Summers, "Tienet: Text-image embedding network for common thorax disease classification and reporting in chest x-rays," in *CVPR*, 2018, pp. 9049–9058.
- [21] M. E. Peters *et al.*, "Deep contextualized word representations," in *Proc. of NAACL*, 2018.
- [22] A. Radford, K. Narasimhan, T. Salimans, and I. Sutskever, "Improving language understanding by generative pre-training," 2018.
- [23] D. Mahapatra and Z. Ge, "Training data independent image registration with gans using transfer learning and segmentation information," in *2019 IEEE 16th International Symposium on Biomedical Imaging (ISBI 2019)*, 2019, pp. 709–713.
- [24] Z. Jiang, H. Zhang, Y. Wang, and S.-B. Ko, "Retinal blood vessel segmentation using fully convolutional network with transfer learning," *Computerized Medical Imaging and Graphics*, vol. 68, pp. 1–15, 2018.
- [25] A. R. Lopez, X. Giro-i-Nieto, J. Burdick, and O. Marques, "Skin lesion classification from dermoscopic images using deep learning techniques," in *2017 13th IASTED International Conference on Biomedical Engineering (BioMed)*, 2017, pp. 1–6.
- [26] M. Raghu, C. Zhang, J. Kleinberg, and S. Bengio, "Transfusion: Understanding transfer learning for medical imaging," in *NeurIPS 2019 : Thirty-third Conference on Neural Information Processing Systems*, 2019, pp. 3347–3357.
- [27] H.-C. Shin *et al.*, "Deep convolutional neural networks for computer-aided detection: Cnn architectures, dataset characteristics and transfer learning," *IEEE Transactions on Medical Imaging*, vol. 35, no. 5, pp. 1285–1298, 2016.
- [28] D. Nie and D. Shen, "Adversarial confidence learning for medical image segmentation and synthesis," *Computerized Medical Imaging and Graphics*, vol. 68, pp. 1–15, 2018.
- [29] Q. Dou, H. Chen, J. Qin, and P.-A. Heng, "Automatic lesion detection with three-dimensional convolutional neural networks," in *BioMedical information technology*. Elsevier, 2020, pp. 265–293.
- [30] R. K. Samala, H. Chan, L. Hadjiiski, M. A. Helvie, C. D. Richter, and K. H. Cha, "Breast cancer diagnosis in digital breast tomosynthesis: Effects of training sample size on multi-stage transfer learning using deep neural nets," *IEEE Transactions on Medical Imaging*, vol. 38, no. 3, pp. 686–696, 2019.
- [31] X. Xu *et al.*, "Deep learning system to screen coronavirus disease 2019 pneumonia," *arXiv preprint arXiv:2002.09334*, 2020.
- [32] M. Z. Alom, M. M. S. Rahman, M. S. Nasrin, T. M. Taha, and V. K. Asari, "COVID_MNet: COVID-19 detection with Multi-Task deep learning approaches," *arXiv preprint arXiv:2004.03747*, 2020.
- [33] Y. Peng, Y.-X. Tang, S. Lee, Y. Zhu, R. M. Summers, and Z. Lu, "Covid-19-ct-cxr: a freely accessible and weakly labeled chest x-ray and ct image collection on covid-19 from biomedical literature," 2020.
- [34] A. Vaswani *et al.*, "Attention is all you need," in *Advances in Neural Information Processing Systems*, 2017, pp. 5998–6008.
- [35] G. Huang, Z. Liu, L. Van Der Maaten, and K. Q. Weinberger, "Densely connected convolutional networks," in *Proceedings of the IEEE conference on computer vision and pattern recognition*, 2017, pp. 4700–4708.
- [36] K. Papineni, S. Roukos, T. Ward, and W.-J. Zhu, "Bleu: a method for automatic evaluation of machine translation," in *Proceedings of the 40th Annual Meeting of the Association for Computational Linguistics*. Philadelphia, Pennsylvania, USA: Association for Computational Linguistics, Jul. 2002, pp. 311–318. [Online]. Available: <https://www.aclweb.org/anthology/P02-1040>
- [37] C.-Y. Lin, "ROUGE: A package for automatic evaluation of summaries," in *Text Summarization Branches Out*. Barcelona, Spain: Association for Computational Linguistics, Jul. 2004, pp. 74–81. [Online]. Available: <https://www.aclweb.org/anthology/W04-1013>
- [38] R. Vedantam, C. Lawrence Zitnick, and D. Parikh, "Cider: Consensus-based image description evaluation," in *CVPR*, 2015, pp. 4566–4575.
- [39] A. Radford, J. Wu, R. Child, D. Luan, D. Amodei, I. Sutskever *et al.*, "Language models are unsupervised multitask learners," *OpenAI blog*, vol. 1, no. 8, p. 9, 2019.
- [40] K. Simonyan and A. Zisserman, "Very deep convolutional networks for large-scale image recognition," *arXiv preprint arXiv:1409.1556*, 2014.



Guangyi Liu received his B.E. degree in Automation Engineering from University of Electronic Science and Technology of China, Chengdu, China, in 2018. He is currently pursuing the Ph.D. degree with the Deep Bit Lab, Future Network of Intelligence Institute (FNii), Chinese University of Hong Kong, Shenzhen, China. His research interests include natural language generation and text variational autoencoder.



Yinghong Liao received the B.E. degree in Software Engineering from the School of Data and Computer Science, Sun Yat-sen University, Guangzhou, China in 2019. He is currently pursuing the Ph.D. degree with the Deep Bit Lab, Future Network of Intelligence Institute (FNii), Chinese University of Hong Kong, Shenzhen, China. His research interests include domain adaptation, meta-learning and multi-modal learning.



Fuyu Wang received his B.E. degree in Software Engineering from the School of Computer Science and Engineering, Sun Yat-sen University, Guangzhou, China, in 2018. He is currently pursuing his Ph.D. Degree in Computer Science with the School of Data and Computer Science, Sun Yat-sen University, Guangzhou, China.



Bin Zhang received his M.M. degree in Southern Medical University, Guangzhou, China, in 2017. He received his M.D degree in the Jinan University, Guangzhou, China, in 2021. His research interests include radiomics and deep learning.



Lu Zhang received her M.M. degree in Southern Medical University, Guangzhou, China, in 2019. She is currently pursuing her M.D. degree in the Jinan University, Guangzhou, China. Her research interests include radiomics and deep learning.



Xiaodan Liang is currently an Associate Professor at Sun Yat-sen University. She was a postdoc researcher in the machine learning department at Carnegie Mellon University, working with Prof. Eric Xing, from 2016 to 2018. She received her Ph.D. degree from Sun Yat-sen University, Guangzhou, China, in 2016, advised by Liang Lin. She has published several cutting-edge projects on human-related analysis, including human parsing, pedestrian detection and instance segmentation, 2D/3D human pose estimation and activity recognition.



Xiang Wan received the B.A. degree in information system from Renmin University, Beijing, China, in 1994, and the M.A. and Ph.D. degrees in computing science from the University of Alberta, Edmonton, AB, Canada, in 2002 and 2006, respectively. He was a Research Assistant Professor with Hong Kong Baptist University, Hong Kong, from 2012 to 2018. He has been working as a Senior Research Scientist with the Shenzhen Research Institute of Big Data, Shenzhen, China, since 2018. And he is also with Guangdong Provincial Key Laboratory of Big Data

Computing, the Chinese University of Hong Kong, Shenzhen, China. He has been mainly working on metaanalysis and statistical learning, particularly in the field of large-scale genomic data analysis. He has published more than 50 articles in many top-tier journals and conferences.



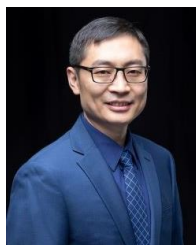
Shaolin Li received the B.M. degree in department of medicine from Air Force Medical University, Xi'an, China, in 1986, and M.M. and M.D. degrees in Imaging and Nuclear Medicine from First Military Medical University, Guangzhou, China, in 1992 and 2007, respectively. He is current a Professor and the Chair of the Department of Imaging Medicine and the Department of Radiology, the Fifth Affiliated Hospital of Sun Yat-sen University, Zhuhai, China.



Zhen Li is currently serving as an assistant professor in the School of Science and Engineering as well as a research scientist in Shenzhen Research Institute of Big data, the Chinese University of Hong Kong, Shenzhen (CUHKSZ). He received his Ph. D. degree in Computer Science from University of Hong Kong (2014-2018), his master degree in Communication and Information Systems from Sun Yat-sen University (2011-2014) and his bachelor degree in Automation from Sun Yat-sen University (2007-2011). He also worked as a visiting scholar in University of Chicago in 2018 and a visiting student in Toyota Technological Institute at Chicago (TTIC) in 2016. His research interests include medical imaging and medical big data, AI interdisciplinary research and computer vision. He has published many papers in top-tier conferences and journals. Meanwhile, he was the core team member for the champion of the 12th Critical Assessment of Protein Structure Prediction (CASP12), with the published paper receiving the PLOS CB 2018 Breakthrough and Innovation Awards and being Web-of-Science Highly Cited paper.



Shuixing Zhang received the B.S., M.S., and Ph.D. degrees from the Department of Radiology, First Military Medical University, Guangzhou, China, in 1993, 2004, and 2007, respectively. He is currently a Professor and the Chair of the Department of Radiology, The First Affiliated Hospital of Jinan University, Guangzhou, China.



Shuguang Cui (Fellow, IEEE) received the Ph.D. degree in electrical engineering from Stanford University, California, USA, in 2005. Afterwards, he has been working as Assistant, Associate, Full, Chair Professor in electrical and computer engineering with the University of Arizona, Texas A&M University, UC Davis, and the Chinese University of Hong Kong, Shenzhen (CUHKSZ), respectively. He has also been the Executive Dean of the School of Science and Engineering, CUHKSZ, and the Executive Vice Director at the Shenzhen Research Institute of Big Data. His current research interests focus on data driven large-scale system control and resource management, large data set analysis, the IoT system design, energy harvesting based communication system design, and cognitive network optimization. He was selected as the Thomson Reuters Highly Cited Researcher and listed in the Worlds' Most Influential Scientific Minds by ScienceWatch in 2014. He was a recipient of the IEEE Signal Processing Society 2012 Best Paper Award. He has served as the general co-chair and TPC co-chairs for many IEEE conferences. He has also been serving as the Area Editor of the IEEE Signal Processing Magazine, and an Associate Editor of the IEEE Transactions on Big Data, IEEE Transactions on Signal Processing, IEEE JSAC Series on Green Communications and Networking, and IEEE Transactions on Wireless Communications. He has been the elected member for IEEE Signal Processing Society SPCOM Technical Committee (2009–2014) and the elected Chair for IEEE ComSoc Wireless Technical Committee (2017–2018). He is a member of the Steering Committee of the IEEE TRANSACTIONS ON BIG DATA and the Chair of the Steering Committee of the IEEE TRANSACTIONS ON COGNITIVE COMMUNICATIONS AND NETWORKING. He was also a member of the IEEE ComSoc Emerging Technology Committee. He was elected as an IEEE ComSoc Distinguished Lecturer in 2014, and IEEE VT Society Distinguished Lecturer in 2019. He has won the IEEE ICC best paper award, ICIP best paper finalist, the First Class Prize in Natural Science from Chinese Institute of Electronics, and the First Class Prize in Technology Invention from the China Institute of Communications all in 2020.